

ACCRETION PROCESSES IN AGN : THE X-RAY VIEW

Christopher S. Reynolds¹

RESUMEN

ABSTRACT

We discuss constraints on the physics of the inner accretion disk, as well as the properties of the black hole itself, that can be derived by a detailed examination of the relativistically broadened spectral features (especially the fluorescent iron line) in the Seyfert galaxy MCG–6-30-15. To begin with, we show that spectral models which purport to eliminate the broad iron line in MCG–6-30-15 by invoking a moderately high ionization absorber are ruled out by recent high-resolution spectra from the *Chandra* High Energy Transmission Gratings. We then discuss the comparison of *XMM-Newton* data with accretion disk models. The “standard” black hole disk model of Novikov, Page and Thorne supplemented by the so-called local corona assumption fails to produce sufficient broadening; this indicates that the real accretion disk in MCG–6-30-15 has significantly more centrally concentrated pattern of X-ray irradiation that predicted by this model. We discuss two possible resolutions. Firstly, the inner disk may be energized from torques imposed by magnetic connections between the disk-proper and either the plunging region or the rotating event horizon itself. Secondly, X-ray emission from a high-latitude source (such as would be the case of the X-ray source is actually the base of a jet) would be gravitationally focused onto the central portions of the disk. We discuss how spectral variability may be used to examine these possibilities and highlight the still outstanding mystery concerning the anti-correlation between the iron line equivalent width and relative normalization of the Compton reflection hump. We end with a few words about the exciting future of these studies heralded by *Constellation-X* and *LISA*.

Key Words: **Keywords go here**

1. INTRODUCTION

More than 40 years ago, it was suggested that the centres of galaxies host supermassive black holes and, further, that accretion onto those black holes powers active galactic nuclei (AGN; Salpeter 1964; Zeldovich 1964; Lynden-Bell 1969). Nowadays, the observational evidence in support of this picture is substantial. Proper motion studies of the stars in the centralmost regions of the Milky Way provide compelling evidence for the presence of a supermassive black hole with a mass of about $3 \times 10^6 M_\odot$ (Eckart & Genzel 1997; Ghez et al. 1998, 2000, 2003; Eckart et al. 2002; Schödel et al. 2002). The kinematics of rotating central gas disks in several nearby low-luminosity AGN has also provided some of the most convincing evidence for supermassive black holes (for example, M87: Ford et al. 1994, Harms et al. 1994; NGC 4258: Miyoshi et al. 1995; Greenhill et al., 1995). Finally, spectroscopic studies of stellar kinematics reveal that almost all galaxies studied to date do indeed possess a central supermassive black hole. The very strong correlation between the stellar velocity dispersion of a galaxy’s bulge and the mass of

the black hole it hosts (Gebhardt et al. 2000; Ferrarese & Merritt 2000) argues for an intimate link between supermassive black hole and galaxy formation, a result of fundamental importance.

With the existence of supermassive black holes established, it is clearly of interest to study them in detail. While of crucial importance for establishing the presence of supermassive black holes, all of the kinematic studies mentioned above probe conditions and physics at large distances from the black hole, $r > 10^3 r_g$, where $r_g = GM/c^2$ and where M is the mass of the black hole. However, the energetically dominant region of an AGN accretion flow is very close to the central black hole, $r < 20 r_g$, where general relativistic effects become strong. This is the region we must consider if we are to truly understand these systems.

Studies of the innermost regions of black hole accretion flows are experiencing an unprecedented confluence of theoretical and observational progress. On the observational side, X-ray spectroscopy of relativistically broadened and distorted emission lines (especially the K-shell transitions of iron) are giving us a relatively clean probe of the region within a few gravitational radii of several AGN black holes

¹Dept. of Astronomy, Univ. of Maryland, College Park, MD 20742, USA

(Tanaka et al. 1995; Fabian et al. 2000; Reynolds & Nowak 2003). These studies will be discussed in more detail in the subsequent sections. Theoretical progress has been equally dramatic. With the realization that magnetohydrodynamic (MHD) turbulence driven by the magneto-rotational instability is the basic driving mechanism for accretion disks around compact objects (Balbus & Hawley 1991), the community is now constructing increasingly realistic, first-principles simulations of black hole accretion disks. For example, current state-of-the-art simulations include the full relativistic effects of a Kerr black hole (De Villiers, Hawley & Krolik 2003), the relativistic mapping of disk emission to a distant observer (Armitage & Reynolds 2004), and accurate treatments of radiation pressure (Turner 2004). In a small number of years, these simulations will be able to give first-principles predictions for directly observable quantities, such as the energy spectrum, temporal power spectrum and coherence function of the emitted radiation.

In this contribution, we discuss the constraints on the nature of the black hole and inner accretion flow that have been derived through X-ray iron line spectroscopy of the intensely studied Seyfert 1.2 galaxy MCG-6-30-15. In particular, we discuss three main results. Firstly, we show that the high-resolution spectrum of MCG-6-30-15 resulting from a half-megasecond observation by the *Chandra* High Energy Transmission Gratings (HETG) gives strong support of the basic broad iron line interpretation of the X-ray spectrum; this spectrum allows us to rule out a model in which the 3-6 keV spectrum curvature (normally interpreted as the redshifted wing of the iron line) is due to ionized absorption mimics a broad iron line. Secondly, we show that black hole spin is required to explain the breadth of the line; a model based on a Schwarzschild black hole requires unphysical distribution of emission across the disk surface. Thirdly, we discuss evidence for the effects of either strong light bending and interaction between the disk and spinning black hole.

2. THE ROBUSTNESS OF BROAD IRON LINES: NEW EVIDENCE FROM HIGH-RESOLUTION SPECTROSCOPY

As we have already mentioned, the principal spectroscopic tool used to date to study strong gravity is the characterization of the broad iron-K α fluorescent emission line (see reviews by Fabian et al. 2000 and Reynolds & Nowak 2003). The essential physics underlying this phenomenon is straightforward. Moderate-to-high luminosity black hole systems accrete via a radiatively-efficient disk. Even

in the region close to the black hole, such a disk will (apart from a hot and tenuous X-ray emitting corona) remain optically-thick, geometrically-thin, almost Keplerian, and rather cold ($T < 10^5$ K for AGN). X-ray irradiation of the surface layers of the disk by the corona will excite observable fluorescence lines, with iron-K α being most prominent due to the combination of its astrophysical abundance and fluorescent yield. This emission line is then subject to extreme broadening and skewing due to the both the normal and transverse Doppler effect (associated with the orbital velocity of the disk) as well as the gravitational redshift of the black hole (see Fig. 1).

Unfortunately, nature appears to conspire to ensure that we never have an entirely “clean” view of a broad iron line. In the AGN realm, broad iron line signatures are usually observed in spectra that also show clear signatures of absorption by circumnuclear photoionized plasma (the so-called “warm absorbers”). This has led some authors to suggest that the “broad iron line feature” is actually X-ray continuum radiation that has been etched away by ionized absorption. Within the context of these pure absorption models, strong curvature is introduced below 7 keV principally by L-shell absorption of intermediate charge-states of iron. Together with the sharp K-shell edge at > 7 keV, these models can produce a broad and asymmetric feature that superficially resembles a broad iron line. Such a model was computed in detail for the case of MCG-6-30-15 by Kinkhabwala (2003) and shown to provide an adequate fit to the time-averaged 350 ks *XMM-Newton* data of Fabian et al. (2002) without any need for relativistic effects.

The Kinkhabwala ionized absorption model for MCG-6-30-15 makes a generic prediction. The immediately ionized states of iron (FeXVII-FeXXIII) producing the L-shell absorption noted above will imprint a set of K-shell resonant absorption lines at 6.4–6.6 keV (see Fig. 2). With the loss of the XRS on *Suzaku*, only the *Chandra*/HETG has the spectral resolution required to search for and characterize these lines. With this goal, we² obtained a 522 ksec HETG observation of MCG-6-30-15; the iron-band analysis of these data was led by Andrew Young and has been reported by us in Young et al. (2005). This spectrum clearly shows a weak rest-frame narrow iron-K α fluorescence line at 6.40 keV, as well as the K-shell resonant absorption lines of helium- and hydrogen-like iron (see Fig. 3, left panel). The highly ionized iron absorption lines are blueshifted

²The *Chandra* observation was made possible through the Guaranteed Time of C. R. Canizares and A. C. Fabian.

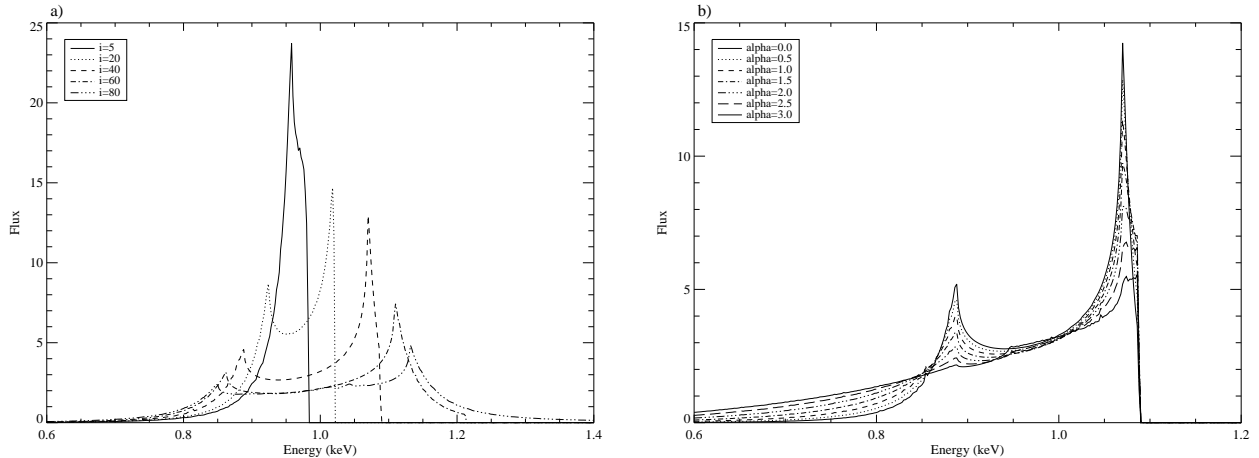


Fig. 1. Calculations of line profiles from a thin Keplerian disk around a Kerr black hole. In these examples, the rest-frame energy of this hypothetical emission line is 1, keV. In all cases shown, the range of emitting radii extends from the radius of marginal stability to $50GM/c^2$. *Left panel* : Variations of line profiles with inclination angle for a radial emissivity proportional to $r^{-1.5}$ in the case of a rapidly-rotating black hole (dimensionless spin parameter $a = 0.998$). *Right panel* : Variations of line profiles with emissivity index α (such that the surface emissivity is $r^{-\alpha}$) for a disk around a black hole with spin $a = 0.5$ viewed at an inclination angle $i = 40^\circ$. All computations have been performed with the new `kerrdisk` code (Brenneman & Reynolds 2006).

by 2000 km s^{-1} and hence can be attributed to a photoionized wind, probably originating from the accretion disk itself. Most notable, however, are the *lack* of absorption lines from intermediate ionization states of iron in this spectrum as predicted by the Kinkhabwala model.

We have performed a direct test of the “broad iron line mimicking warm absorber” model for MCG–6–30–15 as follows. Firstly, we modeled the 3–10 keV spectrum from the 350 ks *XMM-Newton*/EPIC observation with power-law subject to a warm absorber (modeled with the XSTAR photoionization code) parameterized by an ionization parameter ($\xi = L_{\text{ion}}/nr^2$; where L_{ion} is the ionizing luminosity of the source, n is the electron number density of the absorber and r is the distance of the absorbing plasma from the source) and a column density (N_{H}); we also excluded the 6–8 keV range from the fit as this is clearly affected by spectral complexity including a narrow iron line. Best fitting warm absorber parameters are $\log \xi = 2.2 \pm 0.1$ and $\log N_{\text{H}} = 22.6 \pm 0.1$ (cgs units). We then fold the best fitting warm absorber through the *Chandra*/HETG response matrix and compare it to our data (Fig. 3, right panel). The model displays a deep absorption feature at 6.5 keV (rest-frame) which is clearly discrepant with our data. Since these absorption feature originate from the *same ions* that

produces the broad iron line like spectral curvature, they are a generic and unavoidable prediction of this model. Thus, we conclude that we can rule out a Kinkhabwala-like ionized absorption model, further bolstering the claim that we are indeed seeing relativistically broad iron line emission.

So, why do broad iron lines often appear in conjunction with ionized absorption? Many of the AGN displaying extremely broadened X-ray reflection features are believed to be accreting at a significant fraction of their Eddington limit. These are precisely the same systems that would be expected to possess a significant radiatively-driven, photoionized wind; such a wind can be launched from the accretion disk itself or be ablated by the radiation field from the sides of the putative cold, dusty torus of AGN unification schemes. Indeed, analysis of warm absorber features in a sample of AGN observed by the *Chandra*/HETG suggests that the ionized mass outflow rates increase as with increasing Eddington ratio (McKernan, Yaqoob & Reynolds 2006). Thus both broad iron lines and ionized absorbers appear to be part of the phenomenology of moderately rapidly accreting sources.

3. PROPERTIES OF THE BLACK HOLE AND THE INNERMOST ACCRETION FLOW

Having established that the relativistic spectral broadening hypothesis remains robust for the case

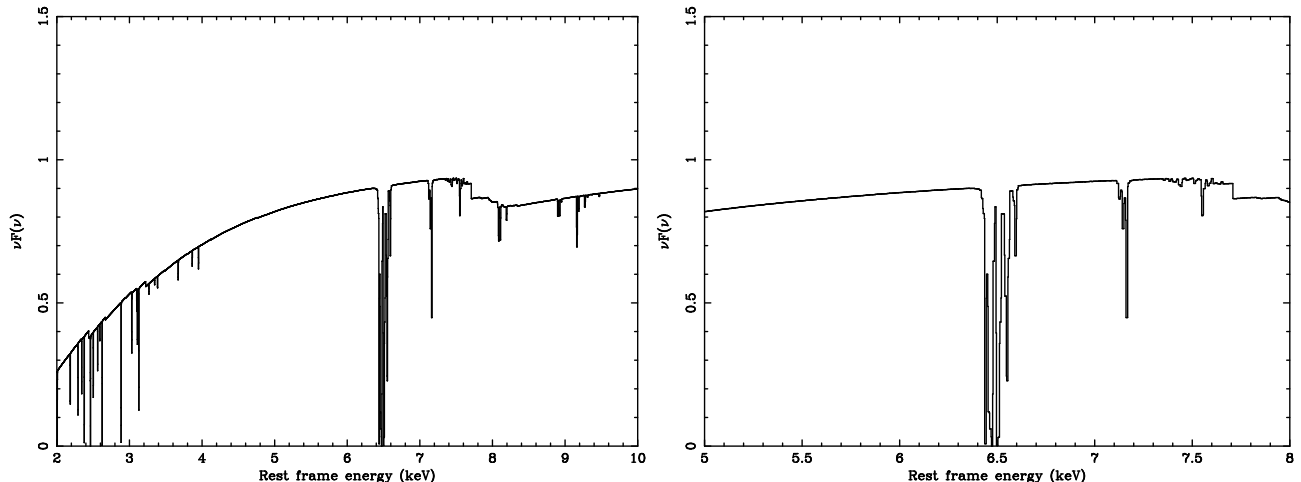


Fig. 2. Example of an ionized absorber model which will mimic a broad iron line when observed at the moderate spectral resolution of the *XMM-Newton*/EPIC. Parameters characterizing this absorber are $\log \xi = 2.2$ and $\log N_{\text{H}} = 22.6$ (cgs units). The underlying powerlaw has a photon index of $\Gamma = 2$ and arbitrary normalization. Note the deep absorption complex at approximately 6.5 keV corresponding to the resonant $K\alpha$ absorption lines of intermediate ionization states of iron. Models have been computed using the XSTAR photoionization code.

of MCG–6–30–15, we will proceed to discuss resulting constraints on the properties of the inner accretion flow and the black hole itself. We begin by discussing constraints on the spin of the black hole. We then proceed to discuss the physics of the innermost regions of the accretion disk and the X-ray source. For the remainder of this section, we shall discuss constraints derived from *XMM-Newton*/EPIC spectroscopy of the broadened X-ray reflection features.

3.1. Black hole spin

There is a common misconception that rapidly spinning black holes *invariably* produce broader and more highly redshifted emission lines than slowly spinning black holes. This stems from the fact that the radius of marginal stability ($6GM/c^2$ for a non-rotating black hole) for a prograde accretion disk pulls-in towards the horizon as the spin-parameter of the black hole is increased. Hence, the line broadening will increase with black hole spin *if* the line emission is always truncated at the radius of marginal stability (see Fig. 4). But it is important to realize that we can produce arbitrarily redshifted and broadened emission lines from around even a non-rotating black hole *if nature had the freedom to produce line emission from any radius beyond the horizon* (Reynolds & Begelman 1997). This discouraging fact has led some authors to conclude that current iron line profiles contain essentially no information on the black hole spin (Dovciak, Karas & Yaqoob

2004).

This would be an overly bleak assessment of our ability to constrain black hole spin. Even the application of some rather weak (i.e., general) astrophysical constraints can impose an inner limit on the radii at which spectral features can be produced. In order to produce any significant iron emission line from the region within the radius of marginal stability (which we shall refer to as the plunging region), the disk in this region must be optically-thick, not too highly ionized (i.e., a significant fraction of the iron cannot be fully ionized), and illuminated by the hard X-ray continuum. While much work remains to be done on the physical state of matter in the plunging region, it is challenging to construct a model for a disk around a non-rotating black hole in which there are appreciable spectral features produced by matter inside of $4.5 - 5GM/c^2$ (Reynolds & Begelman 1997). If we require an emitting radius less than this when fitting a non-rotating black hole model to a particular dataset, we can claim to have found good evidence for a spinning black hole.

This is exactly the situation we find when attempting to fit the *XMM-Newton* data for the Seyfert-1 galaxy MCG–6–30–15. Brenneman & Reynolds (2006) perform a detailed re-analysis of the 350 ks EPIC data (originally presented by Fabian et al. 2002) with a spectral model including a multi-zone dusty warm absorber and a relativistically-blurred reflection spectrum from an ionized accretion

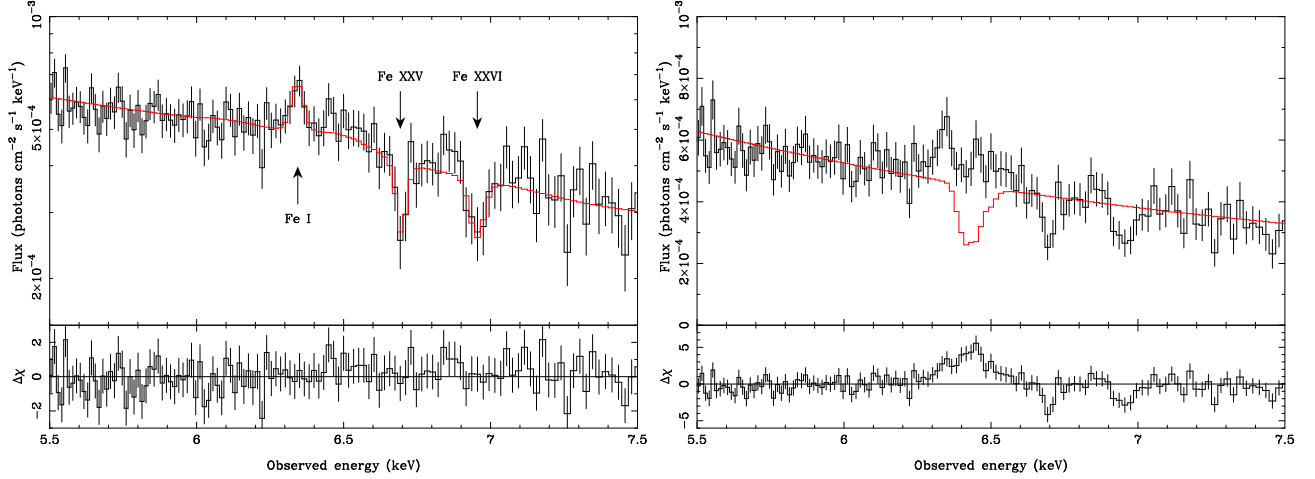


Fig. 3. High-resolution iron band spectrum of MCG-6-30-15 from the *Chandra*/HETG. *Left panel* : HETG spectrum overlaid with a best-fitting model consisting of a power-law continuum, broad iron line (too broad to be seen in this figure), narrow fluorescent line of FeI (at rest with respect to the galaxy), and resonant absorption lines of FeXXV and FeXXVI (blueshifted by $\sim 2000 \text{ km s}^{-1}$ with respect to the galaxy). *Right panel* : HETG spectrum overlaid with a model consisting of a power-law and a warm absorber with column density and ionization state such that it eliminates the red-wing of the iron line in the XMM-Newton/EPIC data. Note the deep absorption feature in the model at 6.5 keV which is clearly absent in the data. Figures from Young et al. (2005).

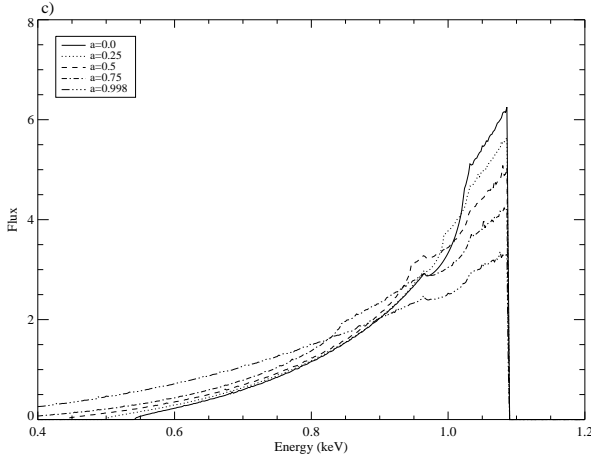


Fig. 4. As for Fig. 1, except showing variations of line profile as a function of black hole spin for an inclination of $i = 40^\circ$ and an emissivity index of $\alpha = 3$ under the assumption that the line emissivity is truncated at the radius of marginal stability. All computations have been performed with the new *kerdisk* code (Brenneman & Reynolds 2006).

disk. They find that, if one *imposes* a Schwarzschild geometry, any adequate fit requires most of the iron line emission to occur at a disk radius of $3GM/c^2$. This is extremely deep within the plunging radius (i.e., the region within the radius of marginal stability at $6GM/c^2$), with radial velocities of the order of half the speed of light expected at that location. Continuity of baryon number demands that the plasma at this location be extremely tenuous. Thus, the irradiating X-rays required to produce the observed X-ray reflection signatures would photoionize this material to an extremely high degree, rendering it incapable of imprinting any atomic features on the spectrum. Thus, we conclude that a Schwarzschild black hole does not allow a physically viable model to be constructed for this spectrum.

In principle, the contribution of the plunging region to the broad iron line profile can be quantified using a detailed model of X-ray reflection from the plunging region which would need to include the effects of finite optical depth and photoionization (Reynolds & Begelman 1997). Significantly more theoretical work is required for these models to stand a chance of describing reality. However, one can illustrate the potential power of broad iron lines to determine black hole spin by the returning to the assumption that there are no X-ray reflection features from the flow within the radius of marginal

stability. As shown by Laura Brenneman elsewhere in this volume, applying spectrum models employing this assumption to MCG-6-30-15 suggests that the black hole is rapidly rotating, $a > 0.93$.

3.2. Confrontation between simple accretion theory and X-ray spectral data

Even before the observational evidence for black hole accretion disks became compelling, the basic theory of such disks had been extensively developed. Building upon the non-relativistic theory of Shakura & Sunyaev (1973), Novikov & Thorne (1974) and Page & Thorne (1974) developed the “standard” model of a geometrically-thin, radiatively-efficient, steady-state, viscous accretion disk around an isolated Kerr black hole. In addition to the assumptions already listed, it is assumed that the viscous torque operating within the disk becomes zero at the radius of marginal stability, $r = r_{\text{ms}}$. Physically, this was justified by assuming that the accretion flow would pass through a sonic point close to $r = r_{\text{ms}}$ and hence flow ballistically (i.e., “plunge”) into the black hole. The zero-torque condition at the radius of marginal stability leads to a predicted dissipation profile which peaks at $r \approx 1.5r_{\text{ms}}$ and then rolls over to zero at the radius of marginal stability.

The Novikov-Thorne disk model gives us a well defined starting point for comparing theory with data. One more step is required, however; we need to relate the underlying dissipation in the accretion disk (given by the Novikov-Thorne model) to the X-ray irradiation of the disk surface (which determines the observed broadening profile of the X-ray reflection spectrum). For the moment, we make the simplest assumption that the primary continuum X-ray source is located a small distance above the disk surface (the “local corona assumption”) and radiates a fixed fraction of the energy dissipated in the underlying disk. This model has been explicitly compared with the first *XMM-Newton* observation of MCG-6-30-15 which caught the source in its enigmatic “Deep Minimum State” (Wilms et al. 2001; Reynolds et al. 2004; see Iwasawa et al. 1996 for the original identification and study of the Deep Minimum State). Reynolds et al. (2004) showed that the “vanilla” Novikov-Thorne model supplemented by the local corona approximation *fails* to produce enough relativistic broadening, even in the case of a near-extremal ($a = 0.998$) rotating black hole (see Fig. 5a). Essentially, there is more X-ray irradiation at the smallest radii compared with the predictions of this model.

One can attempt to rescue the Novikov-Thorne disk model by supposing that a larger portion of the

total dissipation in the disk is channeled into the X-ray emitting corona as one moves to smaller radii. However, since 30–50% of the bolometric power of MCG-6-30-15 seems to emerge through the X-ray emitting corona, one cannot decouple it entirely from the dissipation distribution. In the most extreme model (which provides an adequate but not the best fit to the data), *all* of the dissipated energy is channeled into the X-ray emitting corona within the central $5GM/c^2$, while the X-ray production efficiency is zero beyond that radius.

3.3. Torqued accretion disks

In attempting to reconcile the conflict between data and disk theory noted above, one may consider either modifications to the basic accretion disk dynamics and/or deviations from the local corona assumption. To begin with, we preserve the local corona assumption and examine whether the model can be brought into line with the data via a change of inner boundary condition.

Even when originally setting up the zero-torque boundary condition at the radius of marginal stability, Page & Thorne (1974) noted that magnetic fields may allow this zero-torque boundary condition to be violated. Given the modern viewpoint of accretion disks, that the very “viscosity” driving accretion is due to magnetohydrodynamic (MHD) turbulence, the idea that the zero-torque boundary condition can be violated has been revived by recent theoretical work, starting with Gammie (1999) and Krolik (1999a). In independent treatments, these authors show that significant energy and angular momentum can be extracted from matter within the radius of marginal stability via magnetic connections with the main body of the accretion disk. Agol & Krolik (2000) have performed the formal extension of the standard Novikov-Thorne model to include a torque at $r = r_{\text{ms}}$ and show that the extra dissipation associated with this torque produces a very centrally concentrated dissipation profile. As shown by Gammie (1999), Agol & Krolik (2000), and Li (2002), this process can lead to an extraction (and subsequent dissipation) of spin energy and angular momentum from the rotating black hole by the accretion disk. In these cases, the magnetic forces might be capable of placing the innermost part of the flow on negative energy orbits, allowing a Penrose process to be realized (we note that Williams [2003] has also argued for the importance of a non-magnetic, particle-particle and particle-photon scattering mediated Penrose process). The basic notion that the plunging region exerts significant torques on the disk

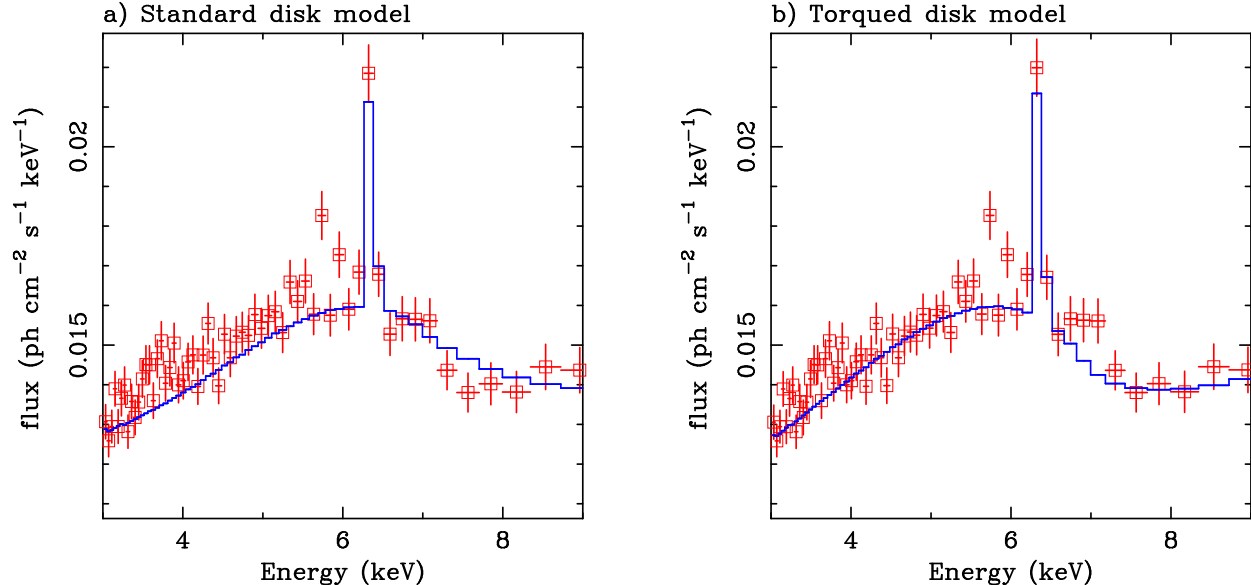


Fig. 5. Broad iron line fit assuming that the line emission tracks the underlying disk dissipation of (a) a standard (Novikov & Thorne 1974) accretion disk and, (b) an Agol & Krolik (2000) torqued accretion disk. Modified from Reynolds et al. (2004).

has been verified through both pseudo-Newtonian (Hawley 2000; Reynolds & Armitage 2001) and fully relativistic MHD simulations of accretion disks (e.g., McKinney & Gammie 2004; Hirose et al. 2004). A second mechanism by which the central accretion disk can be torqued is via a direct magnetic connection between the inner accretion disk and the (rotating) event horizon of the black hole. In this case, as long as the angular velocity of the event horizon exceeds that of the inner disk, energy and angular momentum of the spinning black hole can be extracted via the Blandford-Znajek mechanism (Blandford & Znajek 1977). We note that field lines that directly connect the rotating event horizon with the body of the accretion disk through the plunging region *are* seen in recent General Relativistic MHD simulations of black hole accretion (e.g., Hirose et al. 2004).

Reynolds et al. (2004) has shown that a torqued disk can readily explain the Deep Minimum spectrum provided the source is assumed to be in a torque-dominated state (or, in the terminology of Agol & Krolik [2000], an “infinite-efficiency” state) whereby the power associated with the innermost torque is instantaneously dominating the accretion power (see Fig. 5b). In other words, the X-ray data suggest that during this Deep Minimum state of MCG-6-30-15 the power derived from the black hole spin greatly exceeds that derived from accre-

tion. Of course, this state of affairs cannot last forever or else the central black hole in MCG-6-30-15 would spin down to a point where it could no longer provide this power. At some point in its history, the system must be in an accretion-dominated phase in which the black hole is spun up. However, even in its spin-dominated state, the spin-down timescale of the central black hole is of the order of 100 million years or more. Thus we could envisage a situation in which the system shines via a quasi-steady-state, spin-dominated accretion disk. There are hints, though, that accretion disks may switch between spin-dominated and accretion-dominated on much shorter timescales. In its normal spectral state, the X-ray reflection features in MCG-6-30-15 are much less centrally concentrated than in the Deep Minimum State, suggesting that the normal state might be accretion-dominated. It is also important to note that this system can switch between its normal state and the Deep Minimum State in as little as 5–10 ksec (Iwasawa et al. 1996), which corresponds to only a few dynamical timescales of the inner accretion disk. Thus it is of interest to consider the physics of an accretion disk that undergoes a rapid torquing event.

With this motivation, and guided by the time-variable inner disk torques seen in MHD disk simulations (e.g., Reynolds & Armitage 2001), Garofalo & Reynolds (2005) generalized the torqued-disk

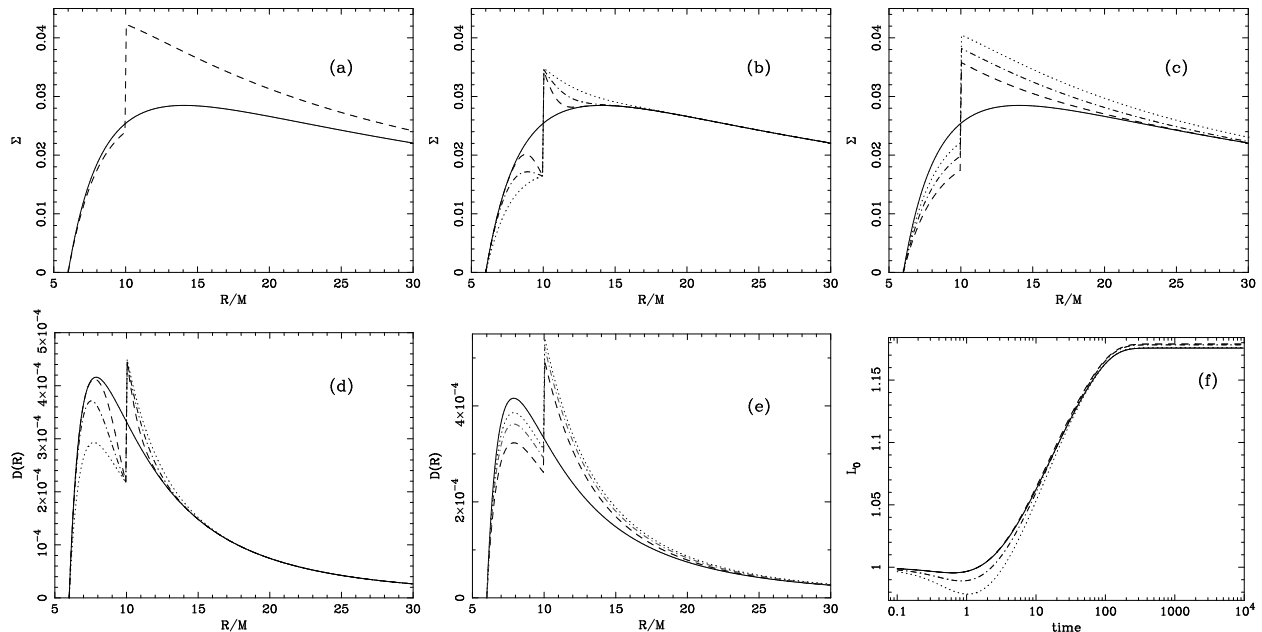


Fig. 6. Evolution of disk in Schwarzschild spacetime for torque at $R/M=10$. Panel (a) shows the surface density profile just after the torquing event begins as well as the steady-state torqued profile is approached (dashed-line: $t = 10000$). Panel (b) shows the early stages in the evolution of the surface density profile with the solid line being the untorqued steady-state profile (dashed-line: $t = 0.8$, dot-dashed-line: $t = 2.53$, dotted-line: $t = 8.0$). Panel (c) shows the untorqued steady-state profile (solid-line) as well as the late-time evolution of the torqued profile (dashed-line: $t = 25$, dot-dashed-line: $t = 80$, dotted-line: $t = 253$). Panel (d) shows the early evolution of the dissipation function with lines and times corresponding to those of panel (b). The qualitative feature is again a drop inward of the torque location and an increase outward. Panel (e) shows the late-time evolution of dissipation function with lines and times analogous to those of panel (c) while panel (f) shows the observed luminosity starting at untorqued steady-state with $t=0$. The observed luminosity is determined for angles of 10 (solid-line), 30 (dashed-line), 60 (dot-dashed line) degrees, and 80 degrees (dotted line). Although the magnitude of the observed luminosity is not the same in the untorqued steady-state for all angles, we have normalized them in order to see the change with respect to the untorqued state. Note the presence of a drop in the luminosity as the angle of inclination decreases. Figures from Garofalo & Reynolds (2005).

models of Agol & Krolik (2000) to include explicit time dependence. They showed that the response of an initially untorqued accretion disk to a sudden (prograde) torquing event has two phases; an initial damming of the accretion flow together with a partial draining of the disk interior to the torque location, followed by a replenishment of the inner disk as the system achieves a new (torqued) steady-state. This is illustrated in Fig. 6 which shows the evolution of the surface density and dissipation profiles for the example of a sporadically torqued disk around a Schwarzschild black hole. Garofalo & Reynolds (2005) propose that some of the spectral changes in MCG-6-30-15 may be due to time-variable magnetic torques between the disk and the plunge region or black hole itself. In particular, they suggest that the extremely centrally concentrated dissipation inferred during the deep minimum state is caused by the on-

set of a strong inner disk torque. To explain why the overall X-ray luminosity of the disk drops during this event (despite the fact that the inner torque is doing work on the disk), Garofalo & Reynolds (2005) suggest that the strong returning radiation associated with this inner torque leads to a Compton-cooling induced collapse of the X-ray emitting corona in all but the innermost regions of the accretion disk.

3.4. Beyond the local corona assumption: the effects of light bending

Another possible explanation for a highly centrally concentrated X-ray irradiation profile is a breakdown of the local-corona assumption. If the X-ray emitting source is a significant height above the optically-thick part of the accretion disk, the hard X-ray continuum photons will be gravitationally focused into the central regions of the accretion disk

(see Andy Fabian’s contribution in these proceedings). Aspects of this scenario have been explored by several authors including Martocchia & Matt (1996), Reynolds & Begelman (1997) and Miniutti & Fabian (2004).

This suggests an alternative picture for MCG-6-30-15 in which the Deep Minimum State is produced when the X-ray source is located at mid/high latitudes very close to the black hole. Reynolds & Begelman (1997) showed that both the changes in the iron line profiles (as then seen by *ASCA*) and the change in the level of the primary continuum can be reproduced by a model in which a fairly constant compact X-ray source on the symmetry/spin axis of the accretion disk is shifting its vertical location. When the source is close to the black hole, the primary X-rays are strongly focused onto the central disk leading to both a very broad line and a diminished observed primary X-ray continuum flux. Miniutti & Fabian (2004) have extended this model and shown that it provides an excellent description of spectral variability seen in all phases of the *XMM-Newton* data for MCG-6-30-15.

We note that the light bending scenario does not diminish the need for exotic spin-related astrophysics — the base of a spin-driven magnetic jet is an obvious candidate for this elevated continuum X-ray source.

3.5. The mysterious variability of the iron line and the Compton reflection hump

While both complex accretion disk dynamics (e.g., magnetic torques between the plunging region and the disk-proper) and light bending of the primary X-ray emission almost certainly are both relevant, it is useful to ask how we might distinguish between these two straw-man models. Spectral variability is likely the key.

Naively, if the geometry of the system and the ionization state of the disk remain unchanged, one expects the fluorescent iron line flux to track the strength of the primary X-ray continuum (i.e., one expected a constant iron line equivalent width). While this is seen in *XMM-Newton* data of MCG-6-30-15 for the low flux states (Reynolds et al. 2004; also see Fig. 7), the iron line *flux* appears to “saturate” at higher fluxes implying that the equivalent width decreases with increasing continuum flux (Fabian et al. 2002). As shown by Miniutti & Fabian (2004), this behaviour has a natural explanation within the light-bending scenario, with the strong light bending changing the effective geometry of the system in just the correct manner. Within

the local-corona, torqued-disk scenario, one needs to posit changes in the ionization state of the surface layers of the disk which conspire to cause an effective saturation of the total line flux.

An equally important but little discussed mystery comes from examining the dependence between the iron line flux and the strength of the Compton reflection hump (seen at 20–30 keV). Naively, assuming a fixed ionization state of the reflector, the iron line equivalent width should be proportional to the relative flux associated with the Compton hump (compared with the direct continuum flux) since both of these spectral features are produced by the X-ray reflection process. The spectral variability in the Miniutti & Fabian (2004) light bending model is primarily due to a change in the fraction of primary X-ray continuum photons are directed into the disk plane and, hence, would predict that this proportionality be preserved. This is not what is observed. Observations by the Proportional Counter Array (PCA) on the *Rossi X-ray Timing Explorer (RXTE)* allows us to measure both the iron line equivalent width and the reflection hump. In a phenomenon first found by Chiang et al. (2000) in NGC 5548, Lee et al. (2001) showed that the iron line equivalent width and the relative normalization of the Compton reflection hump are *anti-correlated*. This result remains valid (and is more generally true for Seyfert 1 nuclei as a class) when the *RXTE*/PCA data are re-analyzed using the latest refinements of the background model and spectral calibration (Mattson, Weaver & Reynolds, in preparation).

If this behaviour is further confirmed (e.g., by *Suzaku*), it will strongly suggest that changes in the ionization state of the accretion disk are playing an important part in determining the spectral variability and must be explicitly modeled.

4. CONCLUSIONS AND FUTURE HOPES

Current data from *XMM-Newton* and *Chandra* are already allowing us to probe black hole physics within a few gravitational radii of the event horizon, and may well be giving us the first observational glimpses of physics within the ergosphere. But this is just the beginning of X-ray astronomy’s exploration of strong gravity and black hole accretion, not the end of the road. The enormous throughput of *Constellation-X* will allow us to probe detailed time variability of the iron line. Dynamical timescale line variability, an easy goal for *Constellation-X*, will allow us to follow non-axisymmetric structures in the disk as they orbit (Armitage & Reynolds 2004; also see Iwasawa, Miniutti & Fabian [2004] for the first

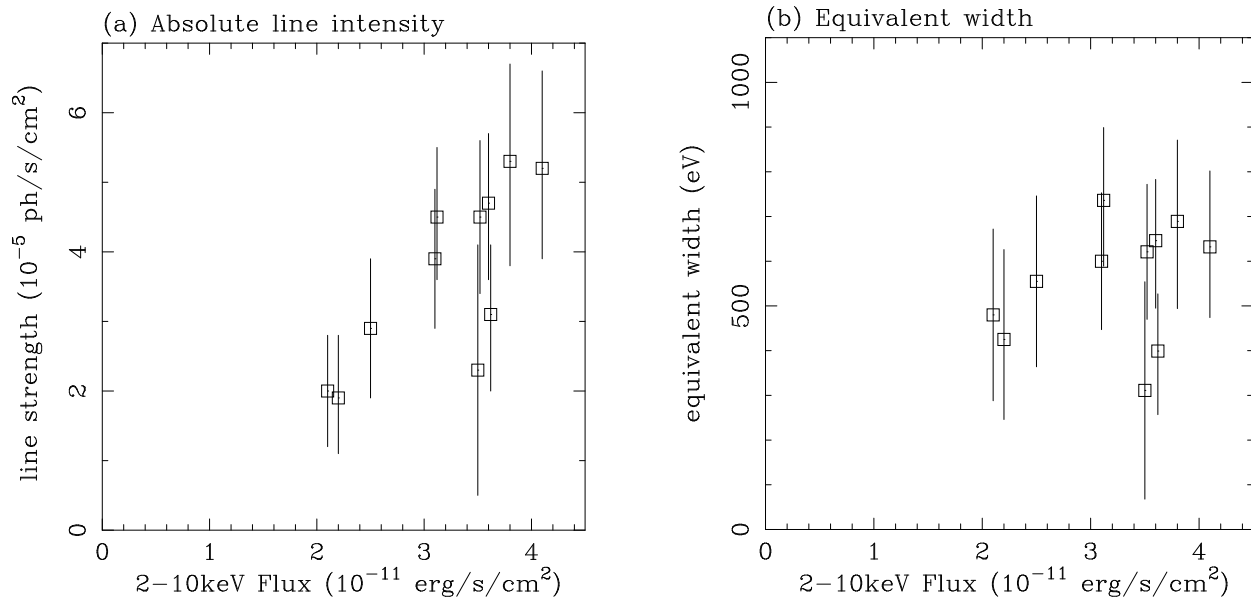


Fig. 7. Result of fitting a simple absorbed power-law plus broad iron line component to the 10 ksec segments of data. Panel (a) shows the absolute intensity of the broad line component as a function of 2–10 keV flux. Note the apparent correlation of line intensity with continuum flux. Panel (b) shows the equivalent width of the *laor* component as a function of 2–10 keV flux. It can be seen that these data are consistent with a constant equivalent width. Error bars are shown at the 90% level for one significant parameter ($\Delta\chi^2 = 2.71$). Figures from Reynolds et al. (2004).

hint of such structure in *XMM-Newton* data). This gives us a direct probe of an almost Keplerian orbit close into a black hole. Furthermore, line variability on the light crossing time will allow us to probe relativistic reverberation signatures (Reynolds et al. 1999; Young & Reynolds 2000), essentially giving us a direct probe of the null geodesics in the space-time. Together, these variability signatures will take their place along side gravitational wave experiments in allowing true tests of strong-field GR.

There is no compelling reason to believe that GR fails on the macroscopic scales probed by either X-ray or gravitational wave studies of astrophysical black holes. In the event that GR is verified, both X-ray and gravitational wave observations will allow unambiguous measurements of black hole spins. Gravitational wave observations with *LISA* of a stellar mass black hole spiraling into a $10^6 M_\odot$ black hole (a so-called Extreme Mass Ratio Inspiral; EMRI) will allow precision measurement of the supermassive black hole’s spin as well as tests of the no-hair theorem and the Kerr metric. X-ray spectroscopy with *Constellation-X* provides a crucial parallel track of study in which we can obtain measurements of black hole spin across the whole mass range of astrophysical black holes (i.e., stellar, intermediate, and su-

permassive) using spectral features that are already known to exist. Only then can the demographics and astrophysical relevance of black hole spin truly be gauged.

We thank the conference organizers for a stimulating meeting. We also thank support from the National Science Foundation under grant AST0205990.

REFERENCES

- Agol, E., Krolik, J.H., 2000, ApJ, 528, 161
- Armitage P.J., Reynolds C.S., 2003, MNRAS, 341, 1041
- Balbus S.A., Hawley J.F., 1991, ApJ, 376, 214
- Blandford, R.D., Znajek, R.L., 1977, MNRAS, 179, 433
- Brenneman L.W., Reynolds C.S., 2006, ApJ, submitted
- Chiang J. et al., 2000, ApJ, 528, 292
- De Villiers J., Hawley J.F., Krolik J.H., 2003, ApJ, 599, 1238
- Dovciak M., Karas V., Yaqoob T., 2004, ApJS, 153, 205
- Eckart A., Genzel R., 1997, MNRAS, 284, 576
- Eckart A., Genzel R., Ott T., Schödel R., 2002, MNRAS, 331, 917
- Fabian, A. C., Iwasawa, K., Reynolds, C. S., & Young, A. J., 2000, PASP, 112, 1145
- Fabian A.C. et al., 2002, MNRAS, 331, L35
- Ferrarese L., Merritt D., 2000, ApJL, 539, L9
- Ford H.C. et al., 1994, ApJL, 435, L27
- Gammie, C.F., 1999, ApJ, 522, 57

- Garofalo D., Reynolds C.S., 2005, *ApJ*, 624, 94
- Gebhardt K., et al., 2000, *ApJL*, 539, L13
- Ghez A., Klein B.L., Morris M., Becklin E.E., 1998, *ApJ*, 509, 687
- Ghez A., Morris M., Becklin E.E., Tanner A., Kremenek T., 2000, *Nature*, 407, 349
- Ghez A. et al., 2003, *ApJ*, 586, L127
- Greenhill L., Henkel C., Becker R., Wilson T.L., Wouterloot J.G.A., 1995, *A&A*, 304, 21
- Harms R.J. et al., 1994, *ApJL*, 435, L35
- Hawley J.F., 2000, *ApJ*, 528, 462
- Hirose, S., et al., 2004, *ApJ*, 606, 1083
- Kinkhabwala A.A., 2003, Ph.D. thesis, Columbia University
- Krolik J.H., 1999, *ApJ*, 515, L73
- Iwasawa, K., et al., 1996, *MNRAS*, 282, 1038
- Iwasawa K., Miniutti G., Fabian A.C., 2004, *MNRAS*, 355, 1073
- Lee J.C., A.C.Fabian, C.S.Reynolds, W.N.Brandt, K.Iwasawa, 2000, *MNRAS*, 318, 857
- Lynden-Bell D., 1969, *Nature*, 223, 690
- Marconi A., Risaliti G., Gilli R., Hunt L.K., Mailino R., Salvati M., 2004, *MNRAS*, 351, 169
- Martocchia A., Matt G., 1996, *MNRAS*, 282, L53
- McKernan, B., Yawoob T., Reynolds C.S., 2006, *MNRAS*, submitted
- Miniutti G., Fabian A.C., 2004, *MNRAS*, 349, 1435
- Myoshi M., Moran J., Herrnstein J., Greenhill L., Nakai N., Diamond P., Inoue M., 1995, *Nature*, 373, 127
- Novikov, I., Thorne K.S., 1973, in *Black Holes*, 1973, ed. C.DeWitt and B.DeWitt(New York: Gordon and Breach)
- Page, D.N., Thorne, K.S., 1974, *ApJ*, 191, 499
- Reynolds, C. S., & Begelman, M. C., 1997, *ApJ*, 487, 109
- Reynolds C.S., Armitage P.J., 2001, *ApJ*, 561, L81
- Reynolds C.S., Nowak M.A., 2003, *Physics Reports*, 377, 389
- Reynolds C.S., Young A.J., Fabian A.C., Begelman M.C., 1999, *ApJ*, 514, 164
- Reynolds C.S., Wilms J., Begelman M.C., Staubert R., Kendziorra E., 2004, *MNRAS*, 349, 1153.
- Salpeter E.E., 1964, *ApJ*, 140, 796
- Schödel R. et al., 2002, *Nature*, 2002, 419, 694
- Shakura, N.I., Sunyaev, R.A., 1973, *A&A*, 24,337
- Tanaka, Y., et al., 1995, *Nature*, 375, 659
- Turner N.J., 2004, *ApJ*, 605, L45
- Williams R.,K., 2003, astro-ph/0306135v1
- Wilms J., et al., 2001, *MNRAS*, 328, L27
- Young A.J., Reynolds C.S., 2000, *ApJ*, 529, 101
- Young A.J., Lee J.C., Fabian A.C., Reynolds C.S., Gibson R.R., Canizares C.R., 2005, *ApJ*, 631, 733
- Zeldovich Y.B., 1964, *Sov. Phys.-Dokl.*, 1548, 811